TISSUE ENGINEERING: Part A
Volume 16, Number 1, 2010

DOI: 10.1089/ten.tea.2009.0255

Osteogenesis and Trophic Factor Secretion are Influenced by the Composition of Hydroxyapatite/Poly(Lactide-Co-Glycolide) Composite Scaffolds

Jiawei He, B.S.,[1] Damian C. Genetos, Ph.D.,[2] and J. Kent Leach, Ph.D.[1]

The use of composite biomaterials for bone repair capitalizes on the beneficial aspects of individual materials while tailoring the mechanical properties of the composite. We hypothesized that substrate composition would modulate the osteogenic response and secretion of potent trophic factors by human mesenchymal stem cells (hMSCs). Composite scaffolds were prepared by combining nanosized hydroxyapatite (HA) and microspheres formed of poly(lactic-co-glycolic acid) (PLG) at varying ratios between 0:1 and 5:1. Scaffolds were seeded with hMSCs for culture in osteogenic conditions or subcutaneous implantation into nude rats. Compressive moduli increased with HA content in a near-linear fashion. The osteogenic differentiation of hMSCs increased in a dose-dependent manner as determined by alkaline phosphatase activity and osteopontin secretion after 4 weeks of culture. Further, endogenous secretion of vascular endothelial growth factor was sustained at significantly higher levels over 28 days for hMSCs seeded in 2.5:1 and 5:1 HA:PLG scaffolds. Eight weeks after implantation, scaffolds with higher HA:PLG ratios exhibited greater vascularization and more mineralized tissue. These data demonstrate that the mechanical properties, osteogenic differentiation, as well as the timing and duration of trophic factor secretion by hMSCs can be tailored through controlling the composition of the polymer–bioceramic composite.

Introduction

Among 6 million fractures occurring each year, 10% exhibit insufficient healing because of improper fixation, metabolic disturbances, or impairment of blood supply, and therefore require further treatment.[1] Such fractures are more likely to occur in the elderly population due to degenerative diseases, including osteoporosis. With >20% of the population over the age of 65 by the year 2025,[2] there is an urgent need for improved bone-healing therapies. Current treatment strategies include autografts, allografts, xenografts, and artificial materials such as metals and bioceramics. Limitations to these strategies such as inadequate tissue supply, potential for disease transfer, compliance issues, and fabrication challenges have cultivated an intense interest in alternatives to these materials.

A host of biomaterials have been examined as potential alternatives to bone grafts, yet each material suffers from limitations that hinder their widespread application. For example, both natural polymers (e.g., collagen and alginate) and synthetic polymers (e.g., aliphatic polyesters such as poly(lactic-co-glycolic acid) [PLG], polycaprolactone, and polyethylene) offer tailorable properties, including porosity and degradability, yet possess poor mechanical properties and lack osteoconductivity. Metals and metal alloys are strong, but are difficult to shape and frequently incompatible with noninvasive imaging modalities. Ceramics including hydroxyapatite (HA) or tricalcium phosphate mimic the natural mineral component of bone while also providing robust mechanical properties and osteoconductivity. However, these materials are brittle and commonly require processing at high temperatures with carefully regulated cooling, thereby complicating the fabrication of constructs to fit nonuniform defect geometries. The implantation of polymer–ceramic composites is a promising approach for addressing the limitations of individual components.

When applied to bone repair, composite scaffolds fabricated from biodegradable polymers and bioceramic compounds aim to maximize the benefits while addressing the limitations of each component. Such composites have been generated using a variety of synthetic polymers and ceramics such as bioactive glasses, carbonate apatite, β-tricalcium

[1]Department of Biomedical Engineering, University of California–Davis, Davis, California.
[2]Surgical and Radiological Sciences, School of Veterinary Medicine, University of California–Davis, Davis, California.

phosphate, and calcium phosphate, and their efficacy in promoting bone repair has been examined in a variety of preclinical studies.[3] These ceramics have varying degradation times, may stimulate osteogenic differentiation, and can be mixed with polymers to generate substrates with gradients in material properties. For example, composites formed of polylactide and calcium phosphate have been assembled into functionally graded implants possessing material properties that vary throughout the substrate and applied for bone repair in the skull.[4]

HA is the primary crystalline component within bone. Synthetic HA may be included in composite biomaterials to capitalize on the contributions of both the highly controllable polymers and mechanically robust and osteoconductive calcium phosphate ceramic.[3] HA-containing composites have been generated from a host of natural and synthetic biodegradable polymers, including chitosan, collagen, polyphosphazene, polyethylene, polycaprolactone, polylactide, and PLG.[5–11] Bioceramic polymer composites can be prepared using a variety of techniques, and the fabrication method directly contributes to the osteogenic response to the constructs.[12] For example, fabrication techniques that conceal the HA from the surface and, hence, the cells in contact with the material may yield improved mechanical properties, but the osteoconductive and osteogenic potential is largely inhibited.

Stem and progenitor cells have tremendous promise for use in regenerative medicine, as they offer a potentially renewable source of almost all cell types participating in bone formation.[13] Mesenchymal stem cells (MSCs), mainly isolated from the bone marrow, increase bone formation upon transplantation, and the subcutaneous implantation of ceramic cubes loaded with progenitor cells has become a standard assay to test the osteogenic potential of stem cells.[14] Regarding cell delivery on other materials, however, it is unclear whether MSCs directly form bone by differentiating into an osteoblastic phenotype, whether they exert trophic effects on neighboring cells, or a combination thereof. MSCs secrete autocrine or paracrine factors that inhibit apoptosis, promote angiogenesis, and stimulate host progenitors to divide and differentiate into varied phenotypes.[15,16] Angiogenesis and neovascularization are critical events in bone repair,[17,18] and trophic factor secretion by MSCs loaded onto composite biomaterials may play a vital role in the success of the ability of these systems to regenerate bone. Indeed, strategies to augment the secretion of endogenous trophic factors would have value for tissue engineering and regenerative medicine applications.

HA-PLG composite scaffolds have recently demonstrated the potential to augment bone repair, in the presence or absence of cells committed to the osteogenic lineage.[11,19] In both studies, the investigators utilized composite substrates with equal mass contributions from the bioceramic (HA) and the polymer (PLG). These materials possess increased wettability, promote osteoconductivity, and act as effective vehicles for implanting cells for bone repair.[11,12,19–21] However, the contribution of HA content to the cellular response was not examined. Therefore, we hypothesized that controlling the mass ratio of HA to polymer would yield a composite scaffold with tailorable material properties that could further promote osteogenic differentiation and trophic factor secretion by human MSCs (hMSCs), thereby resulting in enhanced bone formation.

Materials and Methods

Scaffold fabrication

Scaffolds were prepared using a gas foaming/particulate leaching method as described.[12,22] Briefly, microspheres composed of PLG (8515 DLG 7E; Lakeshore Biomaterials, Birmingham, AL) were prepared using a double-emulsion process.[23] Lyophilized PLG microspheres (8 mg) were mixed with 152 mg of NaCl particles (250–425 μm in diameter) and compressed to a solid disk (final dimensions: 8.5 mm diameter and 1.5 mm thickness; approximately 85 μL total volume) in a custom-made stainless steel die using a Carver press (Fred S. Carver) at 10 MPa for 1 min. An additional 4, 8, 20, and 40 mg of HA nanocrystals (100 nm diameter; Berkeley Advanced Biomaterials) were added to the PLG/NaCl mixture before compression to attain HA:PLG mass ratios of 0.5:1, 1:1, 2.5:1, and 5:1, respectively. Control scaffolds were prepared without HA (0:1). The solid disks were exposed to high-pressure CO_2 gas (5.5 MPa) for at least 16 h to saturate the entire disk. The pressure was rapidly (<1 min) released to ambient, causing the polymer particles to foam and ultimately fuse to create porous polymer matrices. NaCl particles were then removed from the scaffolds by leaching in distilled H_2O over 24 h.

Scaffold characterization

Gross morphology of scaffolds was characterized using scanning electron microscopy. Scaffolds were gold-coated using a sputter coater (Desk II; Denton Vacuum, Moorestown, NJ) and imaged using a scanning electron microscope (Hitachi S3500-N, Pleasanton, CA) at 10 kV. Scaffold porosity was determined using Archimedes' principle as previously described,[24] using a custom-made vacuum bottle and 100% EtOH as the displacement liquid.

Compressive moduli of the scaffolds were determined using an Instron 3345 testing device (Norwood, MA). Scaffolds for each HA:PLG ratio ($n = 9$) were loaded between two flat platens and compressed at 1 mm/min with a preload of 10 N. Compressive moduli were calculated from the linear portion of the force–displacement graph for strain ranging from 0% to 5%.

HA distribution throughout the scaffold was determined by adsorption of trypan blue to each scaffold formulation as described.[12] Scaffolds were exposed to a 0.4% (w/v) solution of trypan blue (Alfa Aesar, Ward Hill, MA) for 10 s. Scaffolds were then rinsed twice in DI H_2O before being placed in 100% EtOH for 1 min. Scaffolds were sonicated for 5 s at 40% power in 100% EtOH to remove remaining unbound dye, and then rinsed in distilled H_2O before drying and analysis.

Detection of fibronectin adsorbed onto HA-PLG scaffolds

The adsorption of fibronectin (FN) onto HA-PLG scaffolds was quantified by Western immunoblotting. Briefly, scaffolds were bisected and incubated for 18 h in human FN (200 μg/mL in phosphate-buffered saline [PBS]; BD Biosciences, San Jose, CA) and washed twice in PBS. Scaffolds were minced with a razor blade, and adsorbed protein was directly lysed in 4× sample buffer (20% glycerol, 4% SDS, 0.05% bromophenol blue, 160 mM Tris-HCl, and 200 mM dithiothreitol (DTT)) supplemented with 0.1% human serum albumin. One microgram of protein per sample was resolved

on 7.5% Tris-HCl acrylamide gels and transferred onto 0.2 mm nitrocellulose. Blots were blocked in 5% nonfat milk in Tris-buffered saline with 0.05% Tween-20 for 1 h and probed with anti-human FN (1:5000 in blocking buffer; sc-11765; Santa Cruz Biotechnology, Santa Cruz, CA) overnight at 4°C. Membranes were washed, and probed with horseradish peroxidase–conjugated secondary antibodies at 1:15,000; reactive bands were observed using enhanced chemiluminescence and X-ray film. Membranes were stripped and probed with anti-human albumin (sc-51515) as a loading control. Films were scanned and imported into Quantity One (Bio-Rad, Hercules, CA), and densitometric analysis was performed.

In vitro *osteogenic potential*

Human bone marrow–derived MSCs (Lonza, Walkersville, MD) were expanded in alpha-modified Eagle's medium (α-MEM) + Glutamax (Invitrogen, Carlsbad, CA) containing 10% fetal bovine serum (JR Scientific, Woodland, CA) and 1% penicillin and streptomycin (Mediatech, Manassas, VA). Culture-expanded MSCs (passages 4–7) were used for both *in vitro* and *in vivo* studies.

After sterilization, MSCs (3.75×10^5) were statically seeded at 8.7×10^6 cells/mL on bisected scaffolds composed of five different HA-PLG ratios (0:1, 0.5:1, 1:1, 2.5:1, and 5:1) and allowed to attach for 2 h. Cell-seeded scaffolds were then transferred to 12-well plates with a 2 mL medium containing standard osteogenic supplements (10 mM β-glycerophosphate, 50 μg/mL ascorbate-2-phosphate, and 10 nM dexamethasone; all from Sigma Chemical, St. Louis, MO). Scaffolds were maintained in a standard cell culture incubator (37°C, 5% CO_2) on an XYZ shaker at 25 rpm for up to 4 weeks, and the medium was changed three times per week.

At 1, 2, and 4 weeks, scaffolds were washed twice in PBS and minced with a razor blade, and cell lysate was obtained by collecting scaffolds in passive lysis buffer (Promega, San Luis Obispo, CA) and sonicated for 5 s. Total DNA was determined in cell lysates ($n = 5$) using the Quant-iT PicoGreen dsDNA kit (Invitrogen). Alkaline phosphatase (ALP) activity was determined from the same lysate using a routine p-nitrophenyl phosphate (PNPP) assay and subsequently measuring the absorbance at 405 nm as previously described.[22] Before scaffold collection, the medium was replaced with fresh medium for 24 h, and the conditioned medium was collected and assayed for secreted osteopontin and vascular endothelial growth factor (VEGF) using commercially available sandwich ELISAs (R&D Systems, Minneapolis, MN).

In vivo *bone formation*

Treatment of experimental animals was in accordance with University of California–Davis animal care guidelines and all National Institutes of Health animal-handling procedures. Skeletally mature 10-week-old male nude rats ($n = 6$) were anesthetized and maintained using an isoflurane/O_2 mixture delivered through a mask. Whole scaffolds (0:1, 1:1, 2.5:1, and 5:1) were statically seeded with MSCs (7.5×10^5 cells per scaffold) as described above. Four pockets were created in the dorsum, and scaffolds (one of each composition to account for interanimal variability) were implanted subcutaneously. One additional animal received four acellular 2.5:1 HA-PLG scaffolds to characterize the contribution of the biomaterial alone. This composition was selected for analysis because of its improved mechanical properties, high porosity, and favorable increases in the expression of osteogenic and proangiogenic markers observed *in vitro*. The incision was closed, and animals were allowed access to food and water *ad libitum*. Eight weeks after implantation, animals were euthanized, and scaffolds were removed, fixed in phosphate-buffered formalin for 24 h, and then moved to 70% EtOH for future analysis and processing. Mineral distribution and bone formation were determined from scaffolds using micro–computed tomography (microCT) and compressive testing, respectively, while scaffolds from the remaining animals were decalcified in EDTA and underwent histological processing.

Qualitative and quantitative three-dimensional analyses of composite implants were determined using microCT (Scan-Co Medical microCT35, Southeastern, PA). Explanted scaffolds were mounted on a turn table with the flat surface placed parallel to the X-ray beam and imaged with a total of 1000 projections shifted automatically over 180° with the X-ray tube operated at 55 KeV and 145 μA. The reconstruction resolution was set to high resulting in a 2048×2048 pixel image matrix. CT images were reconstructed using a standard convolution back-projection procedure with a Shepp and Logan filter. Bone mineral density and bone volume fraction were measured using a HA calibration phantom. Thresholding was set from 421 to 3000 mg HA/cc to discriminate between mineralized and nonmineralized tissue. After microCT analysis, scaffolds underwent compressive testing as described above.

Explanted scaffolds were demineralized in EDTA, paraffin-embedded, and sectioned at 5 μm thickness. Masson's trichrome stains of tissue sections were used to identify collagen distribution within scaffold sections. Tissue sections were also stained with hematoxylin and eosin for general morphology and for vessel quantification. Vessels were quantified by enumerating circular structures, some containing erythrocytes, and the presence of vessels was confirmed with immunohistochemistry of decalcified sections using a commercially available kit (Chemicon, Billerica, MA) for von Willebrand factor.[25,26] Blood vessels within the margins of the entire scaffold ($n = 3$ per condition) were counted manually at 100× magnification and normalized to tissue area with the use of Adobe Photoshop software (Adobe Systems Incorporated, San Jose, CA).

Statistical analysis

Results are expressed as mean ± standard error of the mean, assuming normal distribution of the data sets. Statistical analyses were performed using analysis of variance followed by a Student–Newman–Keuls *post hoc* test, and probability values (p) for significance were calculated; $p < 0.05$ was considered statistically significant.

Results

Addition of HA alters morphological and mechanical properties

To determine the contribution of HA to the mechanical properties of composite scaffolds, we characterized changes

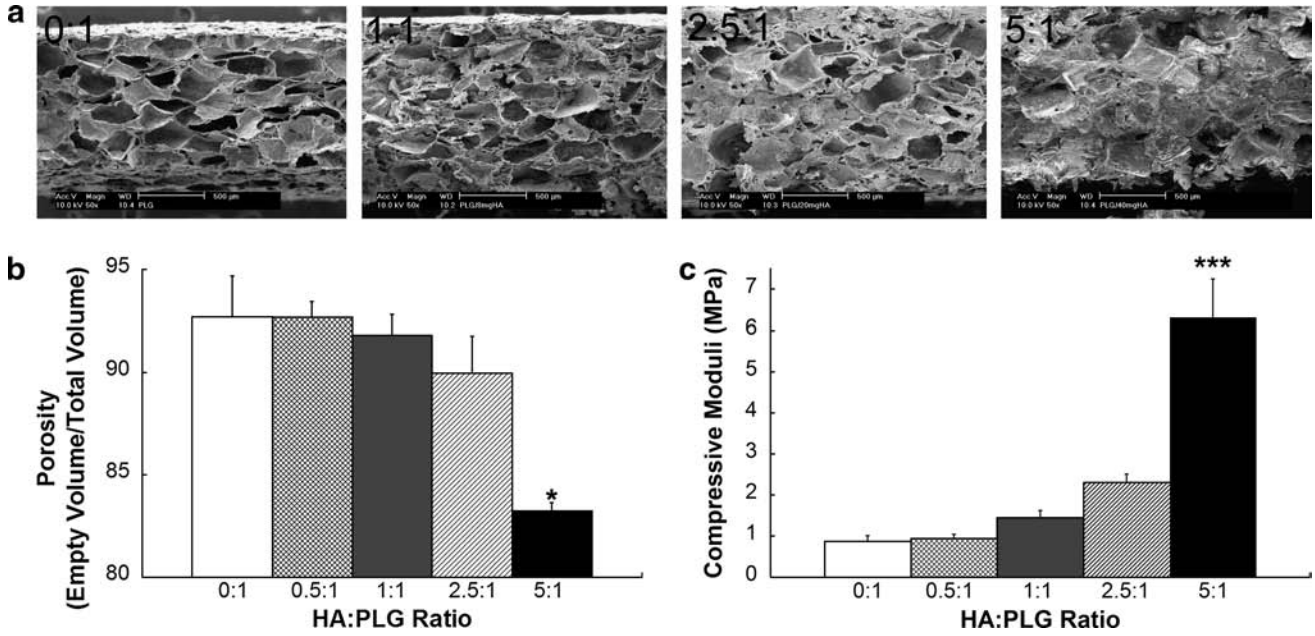

FIG. 1. Influence of HA on porosity and mechanical properties. (**a**) Construct morphology was observed using scanning electron microscopy. (**b**) Scaffold porosity was determined using Archimedes' method ($n = 3$). (**c**) Increases in compressive modulus correlated with increasing HA mass ($n = 9$). *$p < 0.05$ versus all groups. ***$p < 0.001$ versus all groups. HA, hydroxyapatite; PLG, poly(lactic-co-glycolic acid).

in pore size and mechanical properties as a function of HA content. The incorporation of increasing HA mass while keeping PLG mass constant demonstrated a steady decrease in porosity, as determined visually by scanning electron microscopy (Fig. 1a) and Archimedes' method (Fig. 1b). Interestingly, porosity remained high (>90%) for composite scaffolds until 5:1 HA:PLG ($83 \pm 0.4\%$, $p < 0.05$), suggesting that cell viability should not be markedly inhibited using composite scaffolds with HA:PLG ratios up to 2.5:1. Moreover, the macropore structure was largely occluded for 5:1 HA-PLG scaffolds, but the micropore structures were still evident upon examination at higher magnifications (data not shown). This suggests that cell migration into the scaffold may be limited, but the presence of micropores enables the diffusion of nutrients throughout the construct. The reduction in visible macropores and, hence, porosity is caused by a drop in salt weight percent resulting from keeping polymer and salt mass constant with increasing HA mass. As expected, we detected a steady increase in compressive modulus with the addition of HA (Fig. 1c). In fact, we observed a near-linear correlation between HA content and the compressive modulus, thereby demonstrating the tailorability of this method for fabricating composite biomaterials.

Protein adsorption is altered with HA content

We examined the adsorption of a hydrophilic dye, trypan blue, to composite scaffolds as a nonspecific indicator of adsorption potential. Trypan blue does not adsorb well to hydrophobic PLG, but incorporation of increasing HA masses resulted in greater dye adsorption to the composites (Fig. 2a). Further, spreading of the dye was uniform, suggesting that this process generates composites with homogeneous HA distribution.

We next sought to determine whether extracellular matrix proteins differentially adsorbed onto PLG scaffolds with increasing HA content. Fabricated scaffolds were exposed to PBS supplemented with FN, an extracellular matrix component presented to MSCs within an osteogenic milieu, for 18 h. After collection in lysis buffer supplemented with albumin (included as a loading control), samples were analyzed by Western immunoblotting. Little FN was found adsorbed to PLG scaffolds prepared without HA (Fig. 2b), although overexposing the membranes did ultimately reveal immunoreactive bands (data not shown). We observed a trend for increased FN adsorption with increasing HA content. Quantification of these data revealed that the incorporation of HA at ratios of 2.5:1 or 5:1 HA to PLG enhanced FN adsorption by a factor 10.2 ± 3.2 and 7.1 ± 2.2, respectively, compared to PLG scaffolds without HA (Fig. 2c).

Osteogenic potential is modulated by HA content

Our next objective was to determine the potential contribution of HA toward osteogenic differentiation of hMSCs. As early as 7 days and over 4 weeks in culture, we observed that hMSCs could readily deform the scaffolds with low HA content, while those scaffolds with higher HA content remained in their original shape (Fig. 3a). We failed to observe deformation of acellular scaffolds over 28 days in culture, while hMSC-seeded scaffolds maintained in basal media exhibited only slight changes in scaffold morphology.

Cell number was also influenced by the composition of HA:PLG ratios. After 7 days of culture, there were significantly fewer cells in composites containing HA, compared to 0:1 controls (Fig. 3b); this trend persisted after 14 days of culture as well. This was likely a function of porosity differences and resulting influence upon cell number between

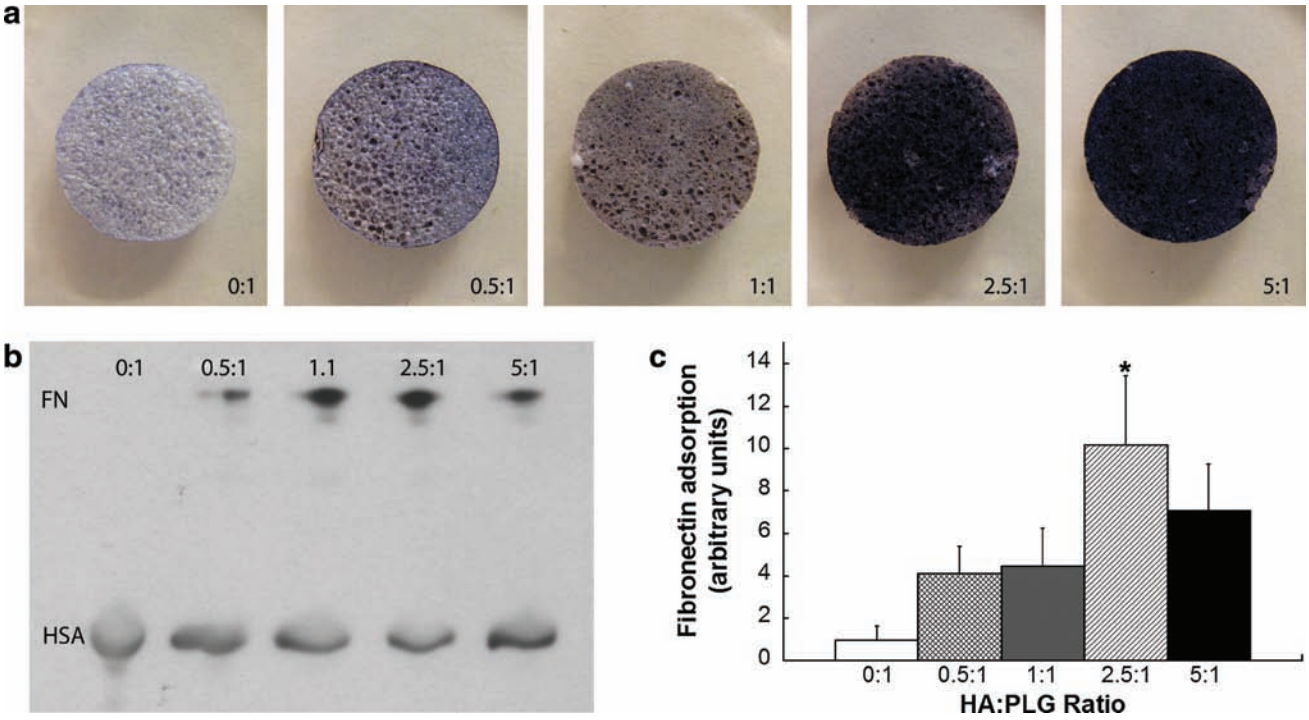

FIG. 2. Incorporation of HA alters adsorption onto PLG scaffolds. (**a**) Increases in trypan blue intensity, coupled with uniform staining of the scaffold, suggest homogeneous distribution of HA for all HA:PLG ratios studied. (**b**) Representative Western blot demonstrating increasing fibronectin (FN) adsorption onto PLG scaffolds of increasing HA content. (**c**) Quantitation of fibronectin adsorption. Bars represent mean fibronectin adsorbed ± standard error of the mean ($n = 6$), expressed as fold change relative to 0:1 in arbitrary units. *$p < 0.05$ compared to 0:1. Color images available online at www.liebertonline.com/ten.

scaffolds. However, cell proliferation was accelerated in the presence of HA compared to the 0:1 scaffolds after 2 weeks of culture, regardless of HA mass, while hMSCs cultured on PLG scaffolds without HA exhibited a steady decline in cell number.

The changes in scaffold morphology and cell number correlated with the detection of early and later markers of osteogenic differentiation. For each time point, there was a clear trend of increased ALP activity (Fig. 3c) and osteopontin secretion (Fig. 3d) with increasing HA:PLG ratios. For a given HA-PLG composition, ALP activity increased over the 4-week culture period. However, osteopontin levels dropped slightly for all HA-PLG scaffolds at 28 days compared to 14 days, potentially owing to the cyclical expression of this osteogenic marker by progenitor cells undergoing osteogenic differentiation.[27]

VEGF secretion is enhanced with HA content

As hMSCs are known to produce trophic factors that drive tissue repair,[16] we quantified the production of VEGF, a potent stimulator of angiogenesis *in vivo*, from hMSCs undergoing osteogenic differentiation on composite scaffolds. During the 4-week culture period, VEGF secretion was enhanced for hMSCs cultured on HA-containing scaffolds, and we observed a trend for increasing magnitudes of VEGF secretion in the presence of greater HA content (Fig. 4). Interestingly, the timing of VEGF secretion was associated with the HA:PLG ratio, with peaks in VEGF production occurring earlier for hMSCs seeded on lower HA:PLG ratios, and higher HA:PLG ratios (e.g., 5:1) exhibited a steadily increasing VEGF production over the culture period.

Neovascularization and bone formation are increased with increasing HA:PLG ratios

Having shown that the osteogenic differentiation and VEGF secretion by hMSCs was influenced by the composition of the scaffold in culture, we next explored whether hMSC-seeded composites of various HA:PLG ratios would yield detectable differences in neovascularization and bone formation. Upon explantation, we consistently observed gross differences in tissue vascularization, with greater HA:PLG ratios associated with enhanced blood vessel invasion. To characterize these observations, blood vessel density in explanted scaffolds was measured (Fig. 5a–c). Increases in vascular density correlated with increasing HA:PLG ratios (Fig. 5d). We observed comparable and significantly increased vessel densities for 2.5:1 and 5:1 HA:PLG ratios (32 ± 5 and 29 ± 4 vessels/mm^2, respectively) compared to 1:1 and 0:1 scaffolds (14 ± 3 and 15 ± 6 vessels/mm^2, respectively). Importantly, we observed robust vascularization at the center of the scaffold, not just near the tissue surface, when implanting hMSCs on composite scaffolds. Acellular 2.5:1 scaffolds induced the lowest vessel density of all groups (11 ± 2 vessels/mm^2), and these vessels were primarily restricted to the peripheral edges of the scaffold, thereby supporting the contribution of hMSCs toward neovascularization.

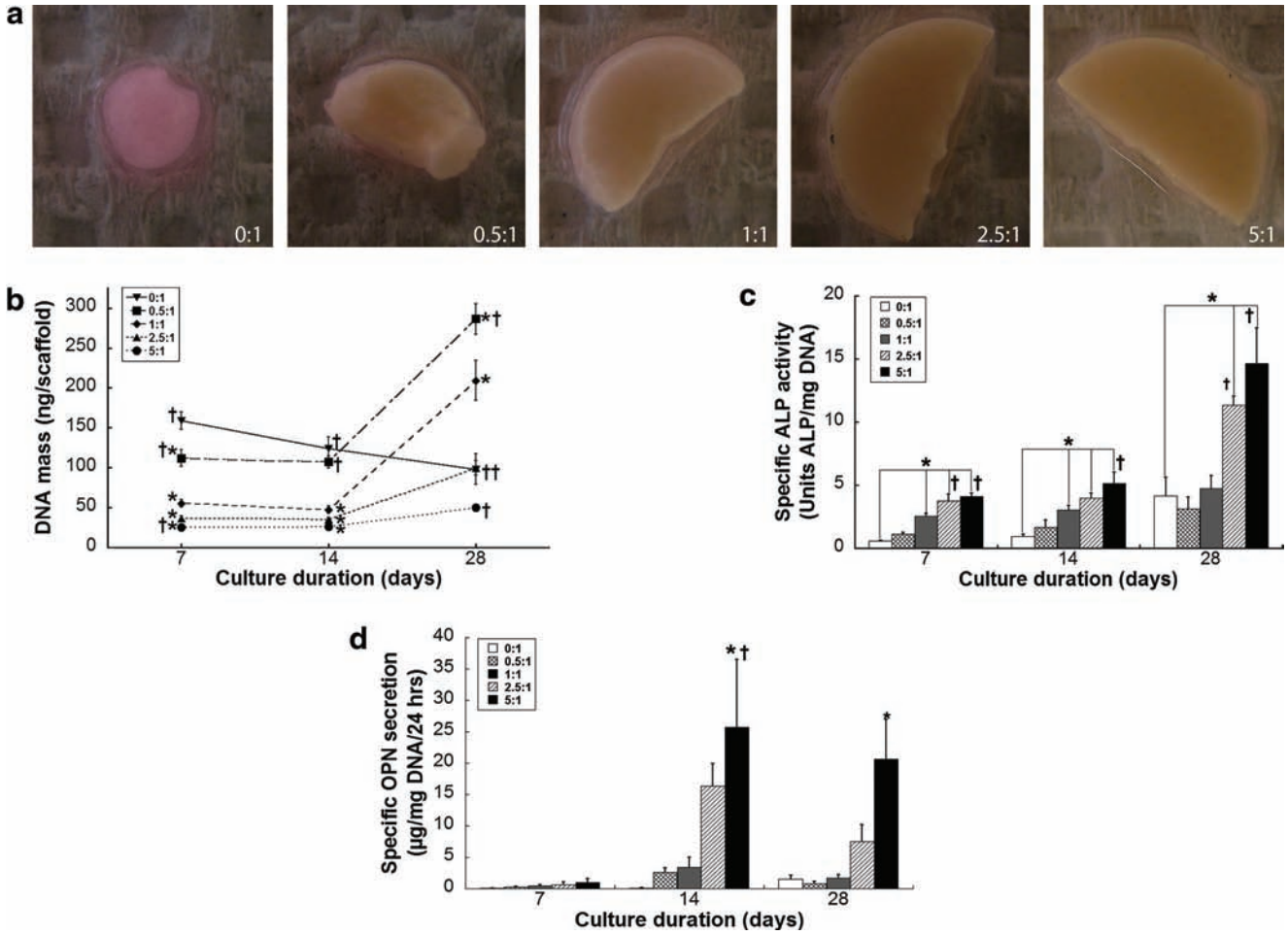

FIG. 3. Contribution of HA to osteogenic differentiation. (**a**) MSC-seeded scaffolds demonstrated clear differences in deformation associated with HA content after 4 weeks in culture. (**b**) Cellular proliferation as a function of scaffold composition. Osteogenic differentiation of MSCs was enhanced with increasing HA:PLG ratios as demonstrated by increasing (**c**) specific alkaline phosphatase activity and (**d**) specific osteopontin secretion ($n = 5$). $^{*}p < 0.05$ versus 0:1; $^{\dagger}p < 0.05$ versus 1:1. MSC, mesenchymal stem cells. Color images available online at www.liebertonline.com/ten.

We also characterized bone formation within scaffolds seeded with hMSCs, as indicated by the presence of mineral using microCT. In agreement with our *in vitro* data (Fig. 3a), scaffolds with little (1:1) or no HA (0:1) were deformed and shrunken, while 2.5:1 and 5:1 composite scaffolds were fully intact upon explantation. As expected, little mineralized tissue was present in scaffolds lacking HA. MicroCT images clearly showed greater mineral distribution with increasing HA:PLG ratios (Fig. 6a). Compared to acellular scaffolds before implantation, we detected significant increases in bone volume fraction for hMSC-seeded scaffolds after 8 weeks (Fig. 6b). These data reflected nearly linear increases in bone volume fraction with regard to the mass of incorporated HA after 8 weeks. Statistically significant increases in bone mineral density were also detected with increasing HA content. Upon explantation, acellular 2.5:1 scaffolds exhibited a bone volume fraction of 0.19 ± 0.01 and bone mineral density of 793.9 ± 2.7 mg HA/cc.

In agreement with microCT analysis, we observed increases in compressive moduli for explanted scaffolds that correlated with HA content (Fig. 6c). These values were lower than acellular scaffolds analyzed *in vitro* (Fig. 1b), thereby confirming that these composite scaffolds underwent substantial degradation while implanted for 8 weeks. Upon examining the developing tissue within decalcified composite scaffolds, the presence of dense connective tissue, suggestive of bone formation, was evident in those scaffolds possessing higher HA content compared to control scaffolds (Fig. 6d). More organized and denser nodes of collagen were apparent in scaffolds with increased HA content (Fig. 6e), while poorly organized collagen was visible for 2.5:1 acellular scaffolds after 8 weeks.

Discussion

In this study, our objective was to gain insight into the role of HA content on bone formation when hMSCs were loaded on polymer–bioceramic composites. When examining *in vitro* osteogenesis in the presence of soluble osteoinductive cues, our data indicate that hMSCs cultured on scaffolds with increasing HA:PLG ratios exhibited enhanced osteogenic differentiation. Previous reports have demonstrated that HA–polymer composites promoted osteogenic differentiation when examining rabbit MSCs, rat osteoblasts, and hu-

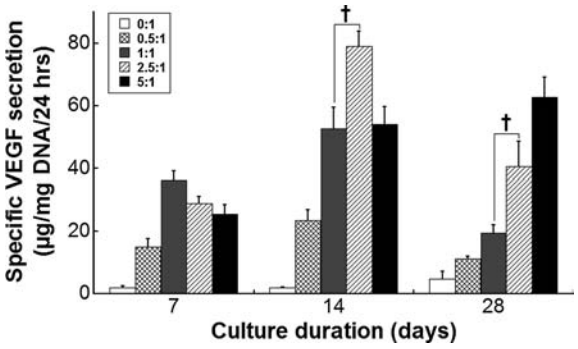

FIG. 4. Contribution of HA to VEGF secretion. The magnitude and timing of VEGF secretion by MSCs was modulated by HA content. Differences in VEGF secretion were significant for all HA:PLG ratios compared to 0:1 ($n = 5$). $^{\dagger}p < 0.05$ versus 1:1. VEGF, vascular endothelial growth factor.

man embryonic stem cell–derived osteogenic cells.[12,19,28] Our motivation for utilizing hMSCs instead of cells more committed to the osteoblastic phenotype is because of the tremendous interest that MSCs have generated in the field of tissue engineering and regenerative medicine. Compared to terminally differentiated cells, MSCs possess increased proliferative capacity and offer a potentially renewable and autologous cell source necessary for bone formation. These data confirm that HA-PLG composite scaffolds can direct hMSC differentiation toward the osteogenic lineage, while also demonstrating that substrate composition can modulate the osteogenic response and, for the first time, trophic factor secretion by associated cells.

Despite convincing evidence of their capacity to form mineralized tissues *in vitro*, the ability of hMSCs to form bone *in situ* is significantly inhibited without an appropriate carrier or in the absence of osteogenic inductive factors such as bone morphogenetic proteins (BMP). Biomaterial-based strategies for directing bone formation offer a number of advantages compared to pharmacological approaches, including localized bone formation, reduced potential to form ectopic bone, and reduced cost. Although effective at bridging bone defects and providing mechanical support, the use of sintered HA, metals, and other osteoconductive materials suffers from poor resorption characteristics and limited malleability, thereby making their widespread application for irregularly shaped defects more challenging.[29]

Resorbable orthopedic biomaterials should possess sufficient porosity to facilitate cellular invasion, enable efficient transport of nutrients to support the survival of cells, and promote integration with surrounding bone. Scaffold porosity was a function of HA content, with substrates maintaining >90% porosity until 5:1 HA:PLG ratio. By keeping PLG and porogen mass constant and only varying HA mass, we generated scaffolds with a wide range of porogen mass percentage by weight, ranging from 95 wt% NaCl in the 0:1 scaffolds down to 76 wt% NaCl in the 5:1 mixtures. Despite these differences in porogen contribution, we failed to appreciate significant differences in porosity, primarily owing to the precision of measurements obtainable by Archimedes' method. The range of porosities may also compromise our

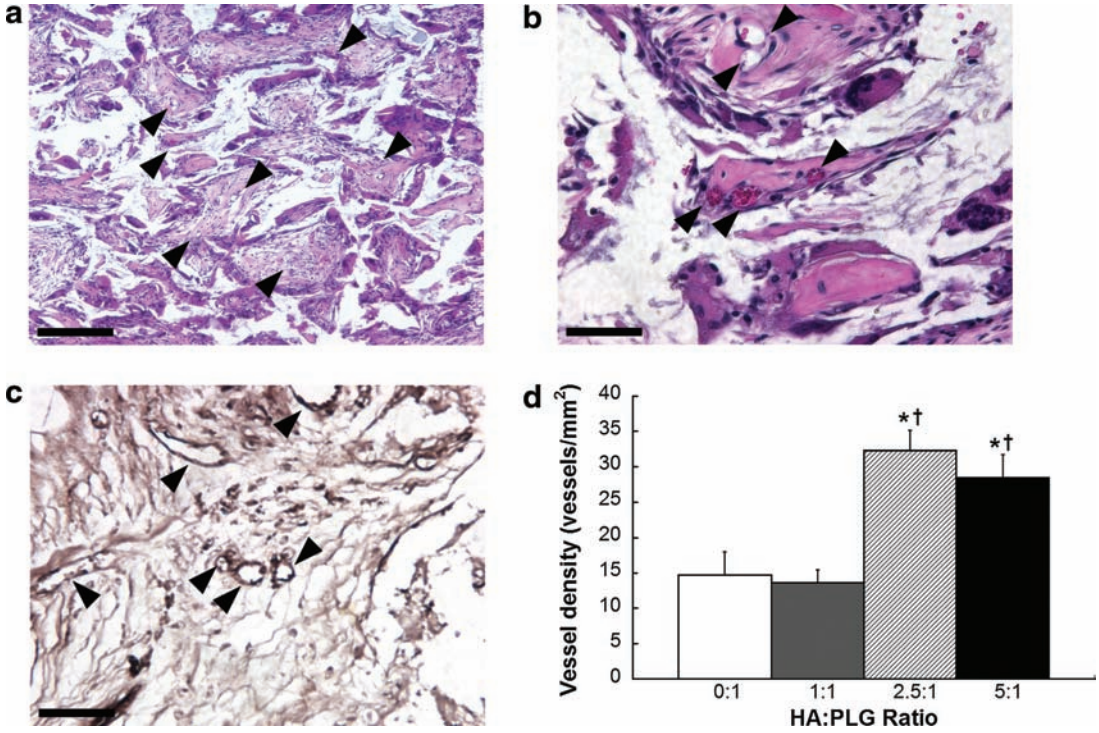

FIG. 5. Neovascularization of composite scaffolds after implantation for 8 weeks. Representative H&E section near the center of explanted scaffolds at 2.5:1 HA:PLG ratio imaged at 10×(**a**) and 40×(**b**). (**c**) Representative immunohistochemistry for von Willebrand factor in 2.5:1 HA-PLG scaffold at 40×. Arrowheads denote vessels; scale bar represents 200 μm (at 10×) and 50 μm (at 40×). (**d**) Vessel counts quantified from H&E sections of explanted scaffolds ($n = 3$ per group). $^{*}p < 0.05$ versus 0:1; $^{\dagger}p < 0.05$ versus 1:1. H&E, hematoxylin and eosin. Color images available online at www.liebertonline.com/ten.

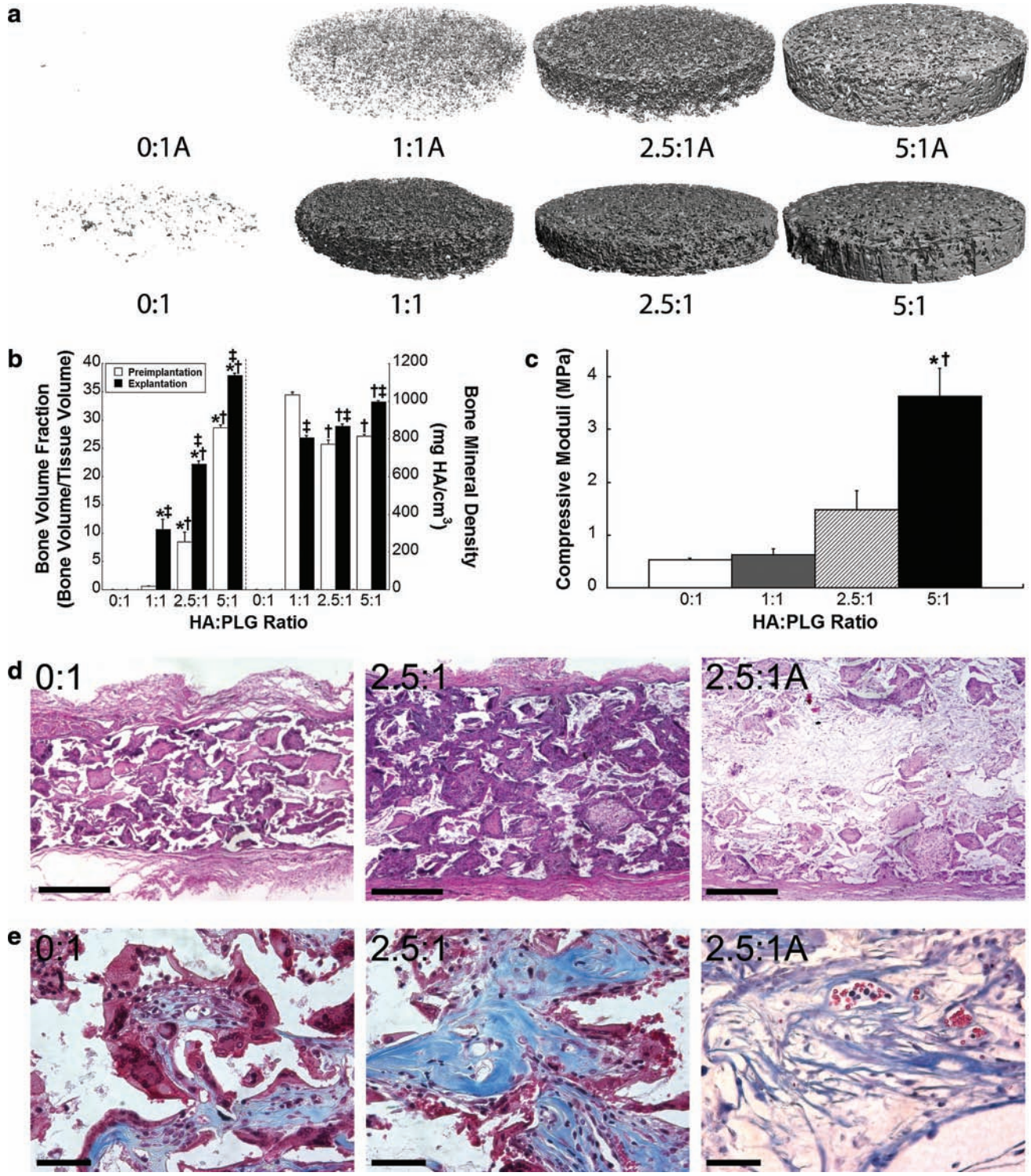

FIG. 6. Bone formation at 8 weeks. (**a**) Differences in mineral coverage are apparent between acellular scaffolds before seeding (top) and explanted scaffolds with micro–computed tomography. (**b**) Bone volume fraction and bone mineral density were determined from micro–computed tomography images for scaffolds preimplantation (open bars) and after explantation (closed bars) ($n = 5$ per group). $^{\ddagger}p < 0.05$ versus preimplantation value; $^{*}p < 0.05$ versus 0:1; $^{\dagger}p < 0.01$ versus 1:1. (**c**) Increases in compressive moduli were detected with increasing HA:PLG ratios after 8 weeks ($n = 3$ per group). (**d**) H&E sections of decalcified explanted scaffolds imaged at 6×demonstrate increased tissue ingrowth and density in 2.5:1 composites versus 0:1 scaffolds, while sections of acellular 2.5:1 scaffolds (2.5:1A) demonstrate reduced tissue ingrowth. Scale bar represents 1 mm. (**e**) Masson's trichrome sections demonstrate increasing collagen coverage with increasing HA content, while acellular sections of 2.5:1 scaffolds exhibit the presence of disorganized collagen. Scale bar represents 50 μm. Color images available online at www.liebertonline.com/ten.

ability to directly compare the mechanical properties for these composite scaffolds. Specifically, substrates with reduced porosities would be expected to exhibit higher moduli, regardless of the presence of mineral, because of the relative reduction in the capacity to compress the scaffold. The reduction in porosity likely leads to exaggerated compressive moduli compared to scaffolds with higher porosities.

The use of HA-PLG composite scaffolds enables control over multiple known elements of osteogenesis. Compared to the relatively hydrophobic PLG, the addition of HA increased the wettability and adsorption of plasma proteins to the substrate. We detected a statistically insignificant ($p = 0.45$) reduction in FN adsorption to 5:1 HA-PLG scaffolds compared to 2.5:1 scaffolds. This result may be due to inefficient initial adsorption at higher HA content as a function of lower porosity, or increased protein binding to the greater HA content that limited complete removal. Biomaterials possess varying affinities for plasma proteins and their associated integrins, and the differential contribution of protein affinity and resultant osteogenic potential of MSCs has been examined for some common polymers.[30,31] Previous studies reported that increased substrate stiffness plays a critical role in the differentiation of MSCs and other cells of the osteoblastic phenotype toward the osteogenic lineage when examined on tailorable hydrogels.[32,33] Despite robust differences in material properties between composite formulations achieved in this study, it is unclear whether the mechanical properties of these composites contribute directly to osteogenic differentiation given that these materials possess significantly greater stiffness values than those examined with other substrates. Although we propose that the inability of MSCs to deform scaffolds with higher HA content is because of increased mechanical properties, one scenario may be that the slow-degrading HA is prolonging the degradation time of composite scaffolds. However, scaffolds with higher HA content possess lower polymer-to-ceramic ratios, thus presenting fewer polymeric connections with HA to degrade and enabling accelerated substrate deformation. We observed scaffold deformation within 1 week of cell culture (far faster than the degradation times of both HA and PLG), suggesting that MSCs are actively seeking to remodel this substrate. The fabrication approach utilized within these studies enables extensive tailorability to potentially match mechanical properties of the substrate with that of the surrounding bone while generating higher compressive moduli. We have incorporated HA masses up to 20 times the polymer mass (20:1 HA:PLG mass ratio), representing an apparent upper limit to generate a contiguous structure by gas foaming. Although we continued to observe increases in compressive moduli (32 ± 2 MPa) for this composition, there is a tremendous sacrifice in porosity ($62 \pm 1\%$) if salt mass remains constant as described in this report.

Angiogenesis and neovascularization are critical processes in bone repair that provide the necessary nutrients and participating cells to heal the defect. A variety of techniques have been applied to promote angiogenesis and resultant bone formation, including the transplantation of vessel-forming cells,[2] biomaterial-based approaches,[25,26] and localized delivery of potent angiogenic inductive factors.[18,25,34] hMSCs are known to secrete trophic factors, including VEGF, that prime the local microenvironment and stimulate tissue formation and repair.[15,16] When hMSCs were seeded on HA-PLG composite scaffolds *in vitro*, the magnitude of VEGF secretion correlated with HA content, and we detected temporal differences in VEGF production as well. In agreement with *in vitro* results, we observed increased vascularization of composites containing 2.5:1 and 5:1 HA:PLG ratios compared to 0:1 and 1:1 HA:PLG scaffolds *in vivo*, potentially because of increased VEGF production over longer durations with larger HA:PLG ratios. We detected widespread distribution of vessels throughout composite scaffolds, including in the center of the substrate. These findings suggest that implantation of hMSCs on these materials is a promising approach to address a key problem in tissue engineering, that being the invasion of blood vessels throughout the developing bone. The endogenous production of VEGF by hMSCs may contribute to assorted potential mechanisms of bone formation in this system, including increased survival and differentiation of hMSCs resulting from increased nutrient availability.[35] Additionally, endothelial cells produce bioactive levels of BMP-2, which may further promote the osteogenic differentiation of MSCs.[36] The increases in vessel density at 8 weeks are particularly impressive in light of the widely reported pruning and regression of newly formed capillaries without vessel-stabilizing signals (platelet-derived growth factor) or mural cells.[37] Importantly, we did not observe the persistence of human cells after 8 weeks after immunohistochemistry for anti-human nuclear antigens, suggesting that transplanted hMSCs participated in neovascularization by secreting trophic factors and did not differentiate into endothelial cells or serve as vessel-stabilizing pericytes.

We determined that composite scaffolds possessing higher HA:PLG ratios yielded more mineralized tissue and maintained their shape and size better than scaffolds with little or no HA. Compared to acellular scaffolds before implantation, clear differences in mineral distribution were evident upon explantation, and we observed significant increases in bone volume fraction for all HA-containing scaffolds. Cell-seeded scaffolds exhibited more thorough mineral distribution and greater occlusion of pores after 8 weeks, suggesting that hMSCs are contributing to new mineral production. Bone mineral density was also significantly increased upon explantation for 2.5:1 and 5:1 HA-PLG scaffolds. However, we detected a reduction in bone mineral density for 1:1 scaffolds after 8 weeks. This difference is attributed to the capacity of microCT to quantify the hardness of individual HA particles with greater dispersion throughout this composition. In general, HA content correlated with increases in bone volume fraction and bone mineral density, while compressive testing was in good agreement with microCT analysis. Indeed, the presence of HA may contribute to both microCT analysis and characterization of compressive strength. Compared to 2.5:1 acellular scaffolds, 2.5:1 scaffolds seeded with hMSCs exhibited significant increases in both bone volume fraction (0.22 ± 0.01 vs. 0.19 ± 0.01; $p < 0.05$) and bone mineral density (867.2 ± 26.5 vs. 793.9 ± 2.7 mg HA/cc; $p < 0.05$). However, we consistently observed lower compressive moduli for implanted hMSC-seeded scaffolds after 8 weeks compared to cell-free scaffolds at day 0. While one might expect the mechanical properties to increase after induction of hMSCs down the osteogenic lineage and resultant mineral deposition, these data are suggestive of extensive polymeric degradation within the composite over 8 weeks. Further, since scaffolds

containing higher HA content possess less PLG per bioceramic on a per mass basis, there is less polymer to degrade (relative to scaffolds with less HA), thus liberating the HA nanoparticles from the contiguous substrate and giving way to tissue invasion, substrate remodeling, and bone formation. Importantly, these data demonstrate that scaffolds with higher HA content continue to exhibit improved mechanical properties over the implantation period. Further, examination of decalcified scaffolds under hematoxylin and eosin staining confirmed the presence of dense connective tissue within scaffolds containing HA.

The fabrication of biodegradable composite scaffolds containing nanosized HA provides an improved composite substrate for use in bone repair. These materials are highly tailorable and malleable, thereby providing clinicians the opportunity to accurately shape the construct and fill irregular-sized defects with a degradable, osteoconductive material to promote bone healing. These composite scaffolds can be cut and shaped within the operating theater to fit the defect margins, and they can be fabricated in any shape provided that the defect is mapped using imaging technology before surgery. Secondly, these composites provide another level of treatment for patients by removing the one-size-fits-all approach and offering the ability to generate bridge materials with similar mechanical properties. Finally, the gas foaming/particulate leaching process used to generate these composites does not require the use of harsh organic solvents or the excessive heat and controlled cooling necessary for fabricating implants such as sintered HA,[38] thereby providing an ideal platform for localized, sustained delivery of osteoinductive factors such as BMP-2 without loss of protein activity. Despite the promise of this approach, these materials fail to provide mechanical strength on par with sintered bioceramics because of the interactions between nanosized HA and polymer, thereby limiting their use to applications that are not fully weight bearing (e.g., craniofacial bone defects and assisted spinal fusion). Further, the potential affinity of growth factors for HA, whether released from the polymer or adsorbed to the bioceramic, may be too great for cells to internalize. These issues merit further investigation to capitalize on the benefits of this hybrid system for use in bone repair.

Conclusions

The results of this study demonstrate the importance of the composition of the delivery vehicle when employing cell-based therapies for bone repair. Using a fabrication process that avoids excessive heat or harsh organic solvents, we produced composite materials that can be tuned with regard to mechanical properties and degradation. This knowledge will provide clinicians increased opportunities to match the mechanical properties of the implantable construct to those of the surrounding tissue. Further, these data demonstrate that scaffold composition is a valuable tool for influencing the timing and duration of trophic factor secretion by hMSCs. This system may have added utility for engineering other tissues in light of the associated proliferative response to HA, enhanced trophic factor secretion, and resultant vessel ingrowth into the construct. Effective vascularization of neotissues is a primary limitation to most *in situ* tissue engineering approaches, and the continued presentation of HA to cells on the surface of biodegradable constructs may provide a novel approach for enhancing angiogenesis without costly growth factors. Lastly, this system may find application as an effective model system to study bone formation *in vitro*.

Acknowledgments

This project was supported by the AO Research Fund of the AO Foundation to J.K.L. (Project no. F-06-98L). In addition, the authors acknowledge financial support from the National Institutes of Health (EB003827 to J.H.).

Disclosure Statement

No competing financial interests exist.

References

1. Logeart-Avramoglou, D., Anagnostou, F., Bizios, R., and Petite, H. Engineering bone: challenges and obstacles. J Cell Mol Med **9,** 72, 2005.
2. Kaigler, D., Krebsbach, P.H., Wang, Z., West, E.R., Horger, K., and Mooney, D.J. Transplanted endothelial cells enhance orthotopic bone regeneration. J Dent Res **85,** 633, 2006.
3. Rezwan, K., Chen, Q.Z., Blaker, J.J., and Boccaccini, A.R. Biodegradable and bioactive porous polymer/inorganic composite scaffolds for bone tissue engineering. Biomaterials **27,** 3413, 2006.
4. Eufinger, H., Rasche, C., Lehmbrock, J., Wehmoller, M., Weihe, S., Schmitz, I., Schiller, C., and Epple, M. Performance of functionally graded implants of polylactides and calcium phosphate/calcium carbonate in an ovine model for computer assisted craniectomy and cranioplasty. Biomaterials **28,** 475, 2007.
5. Zhang, Y., Ni, M., Zhang, M., and Ratner, B. Calcium phosphate-chitosan composite scaffolds for bone tissue engineering. Tissue Eng **9,** 337, 2003.
6. Dawson, J.I., Wahl, D.A., Lanham, S.A., Kanczler, J.M., Czernuszka, J.T., and Oreffo, R.O.C. Development of specific collagen scaffolds to support the osteogenic and chondrogenic differentiation of human bone marrow stromal cells. Biomaterials **29,** 3105, 2008.
7. Nukavarapu, S.P., Kumbar, S.G., Brown, J.L., Krogman, N.R., Weikel, A.L., Hindenlang, M.D., Nair, L.S., Allcock, H.R., and Laurencin, C.T. Polyphosphazene/nano-hydroxyapatite composite microsphere scaffolds for bone tissue engineering. Biomacromolecules **9,** 1818, 2008.
8. Zhang, Y., Tanner, K.E., Gurav, N., and Di Silvio, L. *In vitro* osteoblastic response to 30 vol% hydroxyapatite-polyethylene composite. J Biomed Mater Res A **81A,** 409, 2007.
9. Shor, L., Güçeri, S., Wen, X., Gandhi, M., and Sun, W. Fabrication of three-dimensional polycaprolactone/hydroxyapatite tissue scaffolds and osteoblast-scaffold interactions *in vitro*. Biomaterials **28,** 5291, 2007.
10. Woo, K.M., Seo, J., Zhang, R., and Ma, P.X. Suppression of apoptosis by enhanced protein adsorption on polymer/hydroxyapatite composite scaffolds. Biomaterials **28,** 2622, 2007.
11. Kim, S.S., Ahn, K.M., Park, M.S., Lee, J.H., Choi, C.Y., and Kim, B.S. A poly(lactide-co-glycolide)/hydroxyapatite composite scaffold with enhanced osteoconductivity. J Biomed Mater Res A **80A,** 206, 2007.
12. Kim, S.-S., Sun Park, M., Jeon, O., Yong Choi, C., and Kim, B.-S. Poly(lactide-co-glycolide)/hydroxyapatite com-

posite scaffolds for bone tissue engineering. Biomaterials **27,** 1399, 2006.
13. Pittenger, M.F., Mackay, A.M., Beck, S.C., Jaiswal, R.K., Douglas, R., Mosca, J.D., Moorman, M.A., Simonetti, D.W., Craig, S., and Marshak, D.R. Multilineage potential of adult human mesenchymal stem cells. Science **284,** 143, 1999.
14. Lennon, D.P., and Caplan, A.I. Mesenchymal stem cells for tissue engineering. In: Vunjak-Novakovic, G., and Freshney, R.I., eds. Culture of Cells for Tissue Engineering. Hoboken, NJ: John Wiley & Sons, 2006, pp. 23–59.
15. Haynesworth, S.E., Baber, M.A., and Caplan, A.I. Cytokine expression by human marrow-derived mesenchymal progenitor cells *in vitro*: effects of dexamethasone and IL-1 alpha. J Cell Physiol **166,** 585, 1996.
16. Caplan, A.I., and Dennis, J.E. Mesenchymal stem cells as trophic mediators. J Cell Biochem **98,** 1076, 2006.
17. Street, J., Bao, M., deGuzman, L., Bunting, S., Peale, F.V., Jr., Ferrara, N., Steinmetz, H., Hoeffel, J., Cleland, J.L., Daugherty, A., van Bruggen, N., Redmond, H.P., Carano, R.A., and Filvaroff, E.H. Vascular endothelial growth factor stimulates bone repair by promoting angiogenesis and bone turnover. Proc Natl Acad Sci USA **99,** 9656, 2002.
18. Murphy, W.L., Simmons, C.A., Kaigler, D., and Mooney, D.J. Bone regeneration via a mineral substrate and induced angiogenesis. J Dent Res **83,** 204, 2004.
19. Kim, S., Kim, S.S., Lee, S.H., Eun Ahn, S., Gwak, S.J., Song, J.H., Kim, B.S., and Chung, H.M. *In vivo* bone formation from human embryonic stem cell-derived osteogenic cells in poly(d,l-lactic-co-glycolic acid)/hydroxyapatite composite scaffolds. Biomaterials **29,** 1043, 2008.
20. Kim, S.S., Park, M.S., Gwak, S.J., Choi, C.Y., and Kim, B.S. Accelerated bonelike apatite growth on porous polymer/ceramic composite scaffolds *in vitro*. Tissue Eng **12,** 2997, 2006.
21. Jeon, O., Rhie, J.W., Kwon, I.-K., Kim, J.-H., Kim, B.-S., and Lee, S.-H. *In vivo* bone formation following transplantation of human adipose–derived stromal cells that are not differentiated osteogenically. Tissue Eng **14,** 1285, 2008.
22. Davis, H.E., Rao, R.R., He, J., and Leach, J.K. Biomimetic scaffolds fabricated from apatite-coated polymer microspheres. J Biomed Mater Res A **90,** 1021, 2009.
23. Ennett, A.B., Kaigler, D., and Mooney, D.J. Temporally regulated delivery of VEGF *in vitro* and *in vivo*. J Biomed Mater Res A **79A,** 176, 2006.
24. Yang, J., Shi, G., Bei, J., Wang, S., Cao, Y., Shang, Q., Yang, G., and Wang, W. Fabrication and surface modification of macroporous poly(L-lactic acid) and poly(L-lactic-co-glycolic acid) (70/30) cell scaffolds for human skin fibroblast cell culture. J Biomed Mater Res **62,** 438, 2002.
25. Leach, J.K., Kaigler, D., Wang, Z., Krebsbach, P.H., and Mooney, D.J. Coating of VEGF-releasing scaffolds with bioactive glass for angiogenesis and bone regeneration. Biomaterials **27,** 3249, 2006.
26. Leu, A., Stieger, S.M., Dayton, P., Ferrara, K.W., and Leach, J.K. Angiogenic response to bioactive glass promotes bone healing in an irradiated calvarial defect. Tissue Eng Part A **15,** 877, 2009.
27. Lian, J.B., and Stein, G.S. The developmental stages of osteoblast growth and differentiation exhibit selective responses of genes to growth factors (TGF beta 1) and hormones (vitamin D and glucocorticoids). J Oral Implantol **19,** 95, 1993; discussion 36.
28. Huang, Y.X., Ren, J., Chen, C., Ren, T.B., and Zhou, X.Y. Preparation and properties of poly(lactide-co-glycolide) (PLGA)/nano-hydroxyapatite (NHA) scaffolds by thermally induced phase separation and rabbit MSCs culture on scaffolds. J Biomater Appl **22,** 409, 2008.
29. Hak, D.J. The use of osteoconductive bone graft substitutes in orthopaedic trauma. J Am Acad Orthop Surg **15,** 525, 2007.
30. Chastain, S.R., Kundu, A.K., Dhar, S., Calvert, J.W., and Putnam, A.J. Adhesion of mesenchymal stem cells to polymer scaffolds occurs via distinct ECM ligands and controls their osteogenic differentiation. J Biomed Mater Res A **78A,** 73, 2006.
31. Kundu, A.K., and Putnam, A.J. Vitronectin and collagen I differentially regulate osteogenesis in mesenchymal stem cells. Biochem Biophys Res Commun **347,** 347, 2006.
32. Engler, A.J., Sen, S., Sweeney, H.L., and Discher, D.E. Matrix elasticity directs stem cell lineage specification. Cell **126,** 677, 2006.
33. Khatiwala, C.B., Peyton, S.R., Metzke, M., and Putnam, A.J. The regulation of osteogenesis by ECM rigidity in MC3T3-E1 cells requires MAPK activation. J Cell Physiol **211,** 661, 2007.
34. Kaigler, D., Wang, Z., Horger, K., Mooney, D.J., and Krebsbach, P.H. VEGF scaffolds enhance angiogenesis and bone regeneration in irradiated osseous defects. J Bone Miner Res **21,** 735, 2006.
35. Kaigler, D., Krebsbach, P.H., Polverini, P.J., and Mooney, D.J. Role of vascular endothelial growth factor in bone marrow stromal cell modulation of endothelial cells. Tissue Eng **9,** 95, 2003.
36. Kaigler, D., Krebsbach, P.H., West, E.R., Horger, K., Huang, Y.C., and Mooney, D.J. Endothelial cell modulation of bone marrow stromal cell osteogenic potential. FASEB J **19,** 665, 2005.
37. Richardson, T.P., Peters, M.C., Ennett, A.B., and Mooney, D.J. Polymeric system for dual growth factor delivery. Nat Biotechnol **19,** 1029, 2001.
38. Munar, M.L., Udoh, K., Ishikawa, K., Matsuya, S., and Nakagawa, M. Effects of sintering temperature over 1,300 degrees C on the physical and compositional properties of porous hydroxyapatite foam. Dent Mater J **25,** 51, 2006.

Address correspondence to:
J. Kent Leach, Ph.D.
Department of Biomedical Engineering
University of California–Davis
451 Health Sciences Drive
Davis, CA 95616

E-mail: jkleach@ucdavis.edu

Received: April 15, 2009
Accepted: July 29, 2009
Online Publication Date: September 14, 2009